Neutron decay widths of excited states of ^{11}Be.

Haigh, Peter; Freer, Martin; Ashwood, Nicholas; Bloxham, Thomas; Curtis, Neil; McEwan, Paul; Bohlen, HG; Dorsch, T; Kokalova, Tz; Schulz, Ch; Wheldon, Carl

DOI:
10.1103/PhysRevC.79.014302

Document Version
Publisher's PDF, also known as Version of record

Citation for published version (Harvard):
Haigh, P, Freer, M, Ashwood, N, Bloxham, T, Curtis, N, McEwan, P, Bohlen, HG, Dorsch, T, Kokalova, T, Schulz, C & Wheldon, C 2009, 'Neutron decay widths of excited states of ^{11}Be.', *Physical Review C*, vol. 79, 014302, pp. 1-9. https://doi.org/10.1103/PhysRevC.79.014302

Neutron decay widths of excited states of ^{11}Be

P. J. Haigh,* M. Freer, N. I. Ashwood, T. Bloxham, N. Curtis, and P. McEwan
School of Physics and Astronomy, University of Birmingham, Edgbaston, Birmingham, B15 2TT, United Kingdom

H. G. Bohlen, T. Dorsch, Tz. Kokalova, Ch. Schulz, and C. Wheldon
Hahn-Meitner-Institut, Glienicker Strasse 100, D-14109 Berlin, Germany

(Received 30 July 2008; revised manuscript received 12 December 2008; published 9 January 2009)

The two-neutron transfer reaction ^{9}Be(^{16}O,^{14}O)^{11}Be[^{10}Be + n] has been used to measure the branching ratios for the neutron decay of excited states of ^{11}Be. The ^{14}O ejectile was detected by a Q3D spectrometer at forward angles. The energies and angles of the ^{10}Be fragments of the decaying ^{11}Be* recoil were measured in coincidence with the ^{14}O ejectile using a double-sided silicon strip detector array at backward angles. This enabled a kinematic reconstruction of the reaction to be performed. Theoretical decay branch ratios were calculated using barrier penetrability factors and were compared to the measured ratios to provide information on the relative reduced widths of the states. The decay widths have been used to link states in ^{11}Be with a common structure and structurally to states in the daughter nucleus ^{10}Be. The $3/2^-$ 8.82-MeV state was identified as a candidate for a molecular band head.

DOI: 10.1103/PhysRevC.79.014302 PACS number(s): 21.10.Gv, 21.10.Tg, 25.70.Hi, 27.20.+n

I. INTRODUCTION

The concepts of nuclear clustering and nuclear molecules are best illustrated with the beryllium isotopes. For example, ^{8}Be is an unbound nucleus that has a well-established α-α cluster structure [1,2]. The ^{9}Be ground state has a similar two-center structure but, unlike ^{8}Be, it is bound by 1.67 MeV. The binding energy that stabilizes the system is provided by the extra neutron that resides in delocalized orbits around the α cores. The signature of such a molecular structure is a rotational band, two of which have been identified in ^{9}Be [3–6]; a band built on the $K^\pi = 3/2^-$ ground state (g.s.) in which the valence neutron is in a π-binding orbital and a band built on the $K^\pi = 1/2^+$ first excited state in which the valence neutron is in a σ-binding orbital.

The corresponding molecular structures in ^{10}Be are expected to be dominant just below the $2n + {}^{8}$Be decay threshold. Thus, the molecular structure of the ^{10}Be ground state, which is bound with respect to two neutron emission by 8.48 MeV and to single-neutron decay by 6.81 MeV, is unlikely to be strongly developed. The 5.9583-MeV [2^+], 5.9599-MeV [1^-], 6.1793-MeV [0^+], and 6.2633-MeV [2^-] quartet of states lie much closer to the cluster decay threshold and studies suggest that they may have a molecular structure that is much more pronounced [3–12]. The 1^- and 2^- states have been interpreted as being members of a $K^\pi = 1^-$ rotational band [3–6,13] with the two valence neutrons in a σ-π configuration. Such a rotational connection remains to be experimentally demonstrated, but antisymmetrized molecular dynamics (AMD) calculations suggest a 3^- to 1^- transition rate of $B(E2) = 11.2\ e^2\ \mathrm{fm}^4$ [14] that would provide a useful test of the structure. The 2^+ and 0^+ states have been associated with the π^2 and σ^2 molecular configurations, respectively. The 4^+ member of the rotational band built on the 0^+ state has recently been measured and it was observed [9] to have a well-developed α:$2n$:α molecular structure as predicted.

The structures of the ground states of ^{9}Be and ^{10}Be can be used to examine the structures of the ^{11}Be states with the use of transfer reactions [15–17]. In a $2n$ transfer reaction the molecular structures of the ^{9}Be target nuclei are already preformed and are thus expected to persist in the final nucleus, whereas for a ^{10}Be target the compact structure of the ground state leads to the population of states with a core plus neutron configuration. The population of ^{11}Be states using the one-neutron transfer, ^{10}Be(^{14}N,^{13}N)^{11}Be, and two-neutron transfer, ^{9}Be(^{14}N,^{12}N)^{11}Be, reactions have been measured [18]. For the one-neutron transfer only three excited states were observed to be populated at 0.32, 1.78, and 2.69 MeV, whereas in the two-neutron transfer reaction almost all known states of ^{11}Be up to 25 MeV were observed. Thus, the authors suggested that a rotational band built on the 3.96-MeV [$3/2^-$] state is populated up to high spins [19]. The band was found to have a large moment of inertia that supports the interpretation of a molecular structure with a very large α-α separation of 5–6 fm.

These molecular configurations may also have a connection with halolike structures, because both imply a core plus valence neutrons. For example, it has been suggested that if the core of a halo nucleus such as ^{11}Li undergoes β decay then it is possible for the halo wave function to retain its features after the β decay, despite the fact that the core may now have a rather different structure [20]. Sarazin *et al.* [21] suggested that the 8.82-MeV ^{11}Be state, populated in the β decay of ^{11}Li, is a possible candidate for a two-neutron halo structure that can subsequently survive in a halolike configuration after the neutron decay to ^{10}Be. In this instance the ^{9}Li core undergoes β decay to ^{9}Be and the two valence neutrons remain in the $2s_{1/2}$ orbital. If the β decay proceeds to the ground state of ^{9}Be then this involves a significant structural change of the core; as the rotational band of the ground state of ^{9}Be indicates a large deformation and is consistent with a structure based on

*pjh@np.ph.bham.ac.uk

a $2\alpha + n$ cluster configuration [3–6]. Thus, the two valence "halo" neutrons of the 8.82-MeV state of ^{11}Be would orbit a very different core to the two halo neutrons of the ^{11}Li. This would strongly overlap with a $(1p_{3/2})(2s_{1/2})^2$ shell-model configuration or, in the language of molecular orbitals, two α cores with two neutrons in σ-type molecular orbitals and one neutron in a π orbital. In other words, the two-neutron halo state in ^{11}Be may in fact correspond to a molecular configuration with delocalized covalent neutrons exchanged between the α particles. The decay by emission of a valence neutron would be expected to populate similar molecular/halo states in ^{10}Be. The emission of a $2s_{1/2}$ (σ) neutron from ^{11}Be would be expected to populate the negative-parity states close to 6 MeV in ^{10}Be. In this way the halo and molecular descriptions of this state are not distinct.

To determine the structure of ^{11}Be excited states it is important to study their decay schemes and transition probabilities. Thus, the branching ratios for the neutron decay of excited states of ^{11}Be to states of ^{10}Be has been measured. R-matrix penetrabilities were used to calculate theoretical decay widths for each decay channel available to the excited states. The theoretical and experimentally determined widths are compared to provide information on the relative reduced widths of the states. The decay modes, relative reduced widths, population characteristics, and structures of the ^{10}Be daughter states were used to determine the structure of the ^{11}Be states.

The levels and decay scheme of ^{11}Be have previously been studied through measurements of the β-delayed neutron emission of ^{11}Li [21–27]. Where available, the branching ratios are compared with these measurements. Note that the β-delayed neutron decay spectroscopy method relies on a complicated analysis procedure with a number of ambiguities, whereas the method used here is independent of any measurement of the β-decay branching ratios and relies on the detection of the ^{10}Be fragments, allowing their excitation energy to be obtained so that the decay branches can be measured directly.

II. EXPERIMENTAL PROCEDURE

The two-neutron transfer reaction ^{9}Be(^{16}O,^{14}O)^{11}Be*, ^{11}Be$^* \rightarrow {}^{10}$Be $+ n$ was measured at a beam energy of 234 MeV at the Ionen-Strahl-Labor facility, at the Hahn-Meitner-Institut, Berlin. This reaction has a ground-state Q value of $Q_0 = -21.57$ MeV.

The measurements were performed with a Q3D magnetic spectrometer [28–30] and an array of charged-particle detectors. The angular acceptance of the spectrometer was defined by the entrance slits giving a horizontal range of laboratory scattering angles from 8.5° to 11.5° and a vertical range of ±1.0°. The ^{14}O ejectile was identified in the Q3D focal plane detector using the energy loss (ΔE) of the particles in a gas-filled detector, the energy signal (E) from a scintillator, and the time-of-flight (TOF) of the particles through the spectrometer. The dependence of the TOF of the ^{14}O ejectile on its scattering angle enabled the scattering angle to be measured, see Ref. [31]. Due to the excellent time resolution an angular resolution of 0.3° was achieved. The position of the ^{14}O along the focal plane was measured using the delay-line read-out technique. The ^{14}O nucleus has no bound excited states and thus its position along the focal plane yields the excitation of the ^{11}Be nucleus, as shown in Fig. 1. The resolution [full width at half maximum (FWHM)] of the isolated peak at 1.78 MeV is 0.7 MeV. Hence, the widths observed in the present measurements are dominated by the experimental resolution (see Table I). The reaction target (^{9}Be 200 μg cm^{-2}) had a significant ^{12}C and ^{16}O content. Thus, the measurements of the ^{12}C(^{16}O,^{14}O)^{14}C and ^{16}O(^{16}O,^{14}O)^{18}O reactions were performed on separate targets for background subtraction. The remaining continuous background, in the Q3D focal plane, is due to a three-body process associated with the sequential ^{9}Be(^{16}O,^{15}O$^* \rightarrow {}^{14}$O $+ n$)^{10}Be* reaction. More details regarding the backgrounds and the methods used to fit them to the experimental data can be found in Ref. [31] and the references therein. The scattering angle of the ^{14}O and the excitation energy of the ^{11}Be were used to determine the kinetic energy of the ^{14}O with high precision in the focal plane and thus a complete reconstruction of the binary reaction was performed.

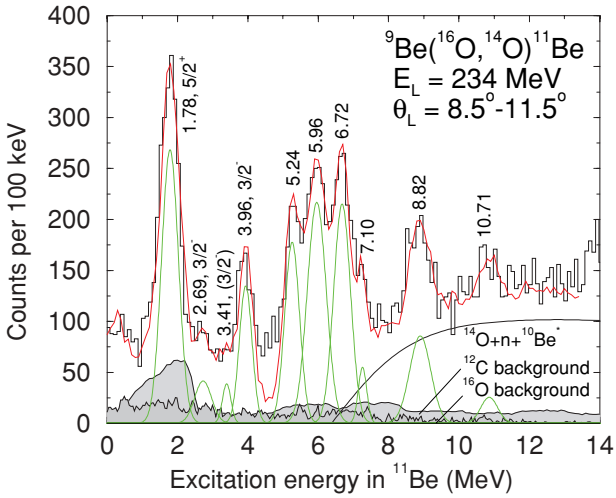

FIG. 1. (Color online) The ^{11}Be excitation energy spectrum fitted with Gaussian peaks (centroids indicated) and a smooth background related to three bodied processes (^{14}O + n + ^{10}Be). The peaks ranging from 0 to 11 MeV represent the ^{11}Be states populated in the two-neutron transfer reaction ^{9}Be(^{16}O,^{14}O)^{11}Be. Background contributions from ^{12}C and ^{16}O target contaminations are labeled. The angular range of the Q3D acceptance aperture is indicated.

The decay products of the excited ^{11}Be recoil were detected, in coincidence with the oxygen ejectile, using an array of four 50 × 50 mm double-sided silicon strip detectors (DSSSD), approximately 500 μm thick. The center of the detectors, with respect to the center of the reaction target, were placed at distances of 142.7, 141.2, 167.3, and 165.8 mm and at angles of 48.9°, 48.3°, 27.3°, and 26.3°, respectively. Each detector face was subdivided into 16 independent 3-mm-wide strips, with the direction of the strips on the front face being perpendicular to those on the back. The detectors had an angular resolution of $\Delta\theta_{\rm lab} \leqslant 1.3°$ and a typical energy resolution of 150 keV (FWHM). The DSSSD also acted as a stop for the TOF of the decay fragments. This technique allowed a kinematic reconstruction of the reaction as well as providing enhanced

TABLE I. Experimental branching ratios for the decay of various ^{11}Be states via the ^{10}Be + n decay channel. The branching ratios are shown for the neutron decay to the 0^+ ground state, the 2^+, 3.3680-MeV first excited state, the quartet of states at ~6 MeV, and the 7.371-MeV [3^-] and 7.542-MeV [2_3^+] states of ^{10}Be. The total widths are taken from Ref. [19].

E_x(^{11}Be) (MeV)	^{10}Be + n				Total width (keV)
	0_1^+	2_1^+	6-MeV group	3_1^-, 2_3^+	
1.78	1.05 ± 0.14				100
3.96	0.48 ± 0.06	0.54 ± 0.07			15
5.24	<0.27	0.81 ± 0.16			40
5.96	<0.13	0.97 ± 0.16			400
6.72	<0.18	0.88 ± 0.15	0.09 ± 0.04		40
8.82	<0.15	<0.06	0.52 ± 0.16	0.59 ± 0.28	200

background suppression. More details about the experimental technique can be found in Ref. [32].

III. ANALYSIS AND RESULTS

Below the two-neutron threshold at 7.316 MeV the only available decay channel for the excited ^{11}Be nucleus is the neutron decay to ^{10}Be ($E_{\text{thresh}} = 0.503$ MeV). Thus, a particle detected in the DSSSD array, in coincidence with a ^{14}O ejectile in the Q3D, was assumed to be a ^{10}Be fragment of the decaying ^{11}Be* nucleus. Momentum conservation was then used to reconstruct the energy and the angle of the undetected neutron and the three-body Q value, Q_3, was calculated as

$$Q_3 = E_{^{14}\text{O}} + E_{^{10}\text{Be}} + E_n - E_{\text{beam}}. \quad (1)$$

The excitation energy of the ^{10}Be was calculated by comparing Q_3 with the three-body Q value in which the decay products are produced in their ground states, Q_{3_0}:

$$E_x(^{10}\text{Be}) = Q_{3_0} - Q_3. \quad (2)$$

The excitation energies of the ^{10}Be fragments were calculated for each individual ^{11}Be state by gating on the appropriate peak in the ^{11}Be excitation energy spectrum (Fig. 1) and a ^{10}Be excitation energy spectrum (Fig. 2) was produced for each decaying ^{11}Be* state. It should be observed that the dominant contribution to the calculated ^{10}Be excitation energy resolution arises from the energy and angular resolution of the silicon array and energy and angular straggling in the target of the recoil-like particles. The missing momentum contribution of the unobserved γ-ray from the decay of the ^{10}Be excited states is small in comparison.

The detection efficiencies of the various neutron decay channels of each individual ^{11}Be state were calculated using Monte Carlo simulations of the reaction and detection processes. The simulations reproduced the experimental

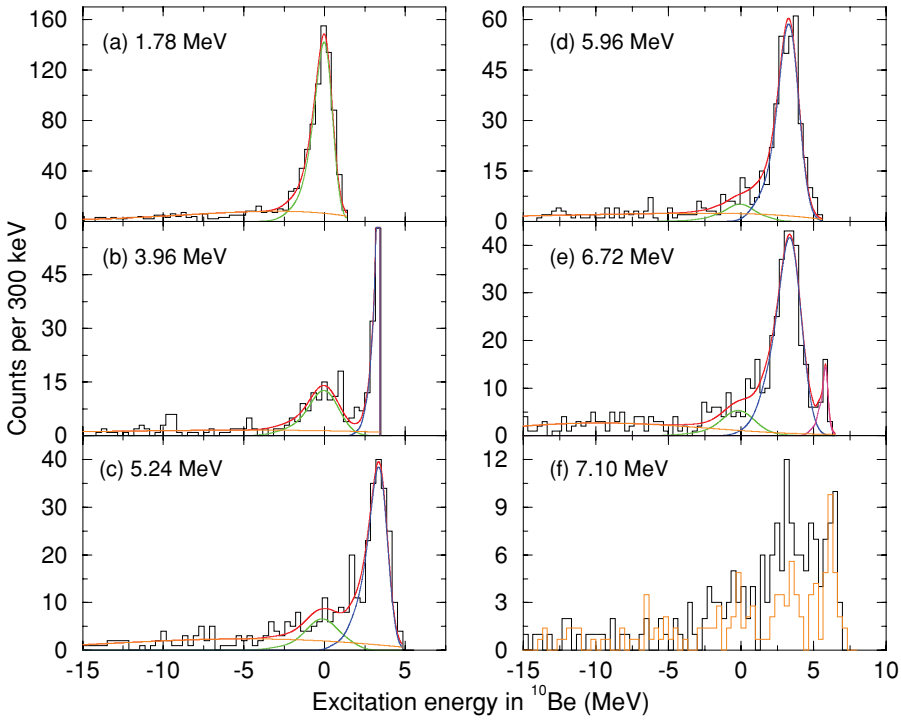

FIG. 2. (Color online) (a)–(e) ^{10}Be states populated in the decay of the excited states of ^{11}Be. The spectra are produced by gating on the appropriate peak in the ^{11}Be excitation energy spectrum (Fig. 1) following the coincident detection of the ^{14}O ejectile and the ^{10}Be fragment and assuming a missing neutron. The data are fitted with the simulated peak line shapes and a smooth polynomial background. In each spectrum the excitation energy of the decaying ^{11}Be state is indicated. (f) The ^{10}Be excitation energy spectrum gated on the 7.10-MeV peak (black histogram) together with the spectrum corresponding to a gate immediately above the 7.10-MeV peak in Fig. 1 (orange histogram).

acceptances and smeared the energies and angles in accordance with the experimental resolutions. The outputs of the simulations were subsequently processed as if they were real events using the same analysis procedures as those used for the experimental data. These simulations permitted the theoretical peak line shapes in the decay products excitation energy spectra to be reconstructed. Figure 2 shows the ^{10}Be states populated in the decay of various ^{11}Be states. The black histograms correspond to the experimental data that has been fitted with the normalized theoretical peak line shapes and smooth polynomial backgrounds. The integrated areas of the normalized peak line shapes were compared with the number of counts in the associated states in the Q3D, ^{11}Be, excitation energy spectrum (Fig. 1) to deduce branching ratios for the neutron decay of the excited states of ^{11}Be to the states of ^{10}Be. The peaks in Fig. 1 were fitted with Gaussian line shapes with widths reflecting the experimental resolutions.

The absolute branching ratio, BR, is the ratio between the decay rate, N_A, of an individual decay channel of a particular ^{11}Be state and the total decay rate, N_T, of that state and is

$$\mathrm{BR} = \frac{N_A/\varepsilon_A}{N_T} = \frac{\text{No. of counts in DSSSD}/\varepsilon_\mathrm{A}}{\text{No. of counts in Q3D detector}}, \qquad (3)$$

where ε_A is the detection efficiency obtained from the Monte Carlo simulations. Note that the detection efficiency is affected only by the dead areas between the detectors as the entire angular distribution of the ^{10}Be fragments falls within the limits of the DSSSD array. Typically the detection efficiencies were around 60%. The value of N_T, for the ^{11}Be state being studied, is given by the number of counts in the relevant peak, in the ^{11}Be excitation energy spectrum (Q3D counts). The value of N_A is given by the number of counts in the associated peak, in the decay fragments excitation energy spectrum (DSSSD counts). The number of counts in a peak was calculated by integrating the normalized function that corresponds to the peak line shape. The branching ratios of ^{11}Be states are shown in Table I.

The 1.78-MeV ^{11}Be state has sufficient excitation energy only to neutron decay to the ground state of ^{10}Be. Thus, this state provides a good method for testing the validity of the procedure used to calculate the branching ratios. Using Eq. (3), the absolute branching ratio for this decay is 1.05 ± 0.14. Thus, within errors, the absolute branching ratio is equal to unity, as expected.

The 3.96-MeV peak in the ^{11}Be excitation energy spectrum of Fig. 1 can be associated with the 3.89- and 3.96-MeV states. However, Bohlen *et al.* [33] showed that the state populated in the ^{9}Be(^{16}O,^{14}O)^{11}Be reaction is the 3.96-MeV state of ^{11}Be. This state has a substantial width for neutron decay to both the ^{10}Be 0^+_1 ground state and the 2^+_1 first excited state.

The 5.24-, 5.96-, and 6.72-MeV states favor the neutron decay to the 2^+_1 state. For these states the decay to the ground state is relatively weak and the associated peak is poorly resolved. In addition to this the ^{12}C(^{16}O, ^{14}O)^{14}C[^{13}C + n] reaction contributes to small even backgrounds in the regions of the ground-state peaks of Fig. 2. Consequently, these branching ratios are listed as upper limits and are expected to be smaller. The 6.72-MeV state also has sufficient excitation energy to decay to the 2^+_2, 1^-_1, and 0^+_2 trio of ^{10}Be states at ~6 MeV. The state is seen to decay with a small branch to a state (or states) at ~6 MeV. However, the decay to the individual states is unresolved due to the experimental resolution.

From Fig. 1 it is clear that the 8.82-MeV peak lies on a three-body background associated with the ^{9}Be(^{16}O,^{15}O$^* \rightarrow$ ^{14}O + n)^{10}Be*(~6 MeV) sequential reaction. An analysis of the coincidence data reveals that the ^{14}O + n decays come from a region close to the associated ^{15}O$^* \rightarrow$ ^{14}O + n decay threshold. This three-body background leads to events in which the ^{10}Be recoil is detected in the DSSSD array in coincidence with an ^{14}O in the Q3D. These events cannot be distinguished from those of the desired reaction channel in which a ^{10}Be is detected following the decay of the excited ^{11}Be recoil. Thus, for the 8.82-MeV state it is necessary to subtract the background in the ^{10}Be excitation energy spectrum that results from the coincident detection of background events in the Q3D and background events in the DSSSD array.

The approximate shape of this background contribution was determined by analyzing the region of the ^{11}Be excitation energy spectrum that lies between the 8.82- and 10.71-MeV peaks and contains only background events. This region was analyzed as a 9.97-MeV ^{11}Be state (mean energy of events in this region) and coincident hits in the DSSSD array were used to produce a ^{10}Be excitation energy spectrum. The histogram showed the shape of the background contribution that arises from the coincident detection of background events. The line shape of this histogram was normalized to fit the 8.82-MeV data by comparing the number of Q3D background events in the 8.82-MeV peak with the number of Q3D background events in the region that was analyzed as a 9.97-MeV peak. This enabled the background in the ^{10}Be excitation energy spectrum to be subtracted.

The 7.10-MeV state also lies in a region where the ^{9}Be(^{16}O,^{15}O$^* \rightarrow$ ^{14}O + n)^{10}Be*(~6 MeV) sequential reaction contributes. In this case the magnitude of the backgrounds compared with the peak strength means that the extraction of branching ratios is more problematic. Figure 2(f) shows the spectrum corresponding to the decay of the 7.10-MeV state (black histogram) together with an orange histogram that corresponds to gating on the ^{11}Be spectrum immediately above the 7.10-MeV peak (with a gate of the same width). There appears to be an excess of counts in the region corresponding to the ^{10}Be 2^+_1 state indicating that this decay branch is preferred.

Figure 3 shows the ^{10}Be excitation energy spectrum associated with the decay of the 8.82-MeV ^{11}Be state after background subtraction. This state has sufficient excitation energy to neutron decay to the 3^-_1 7.37-MeV and 2^+_3 7.54-MeV states of ^{10}Be, which lie above the ^{9}Be + n decay threshold (6.8121 MeV). A ^{10}Be nucleus emitted in one of these excited states will subsequently neutron decay to ^{9}Be. In such decays, the ^{9}Be nuclei detected in the DSSSD array are analyzed as ^{10}Be nuclei. Thus, these events contribute to a ^{9}Be background in the ^{10}Be excitation energy spectrum. Monte Carlo simulations were used to reproduce the line shape of the ^{9}Be background, in the ^{10}Be excitation energy spectrum, which results from these sequential two neutron decays. The line shape was normalized to fit the experimental data and

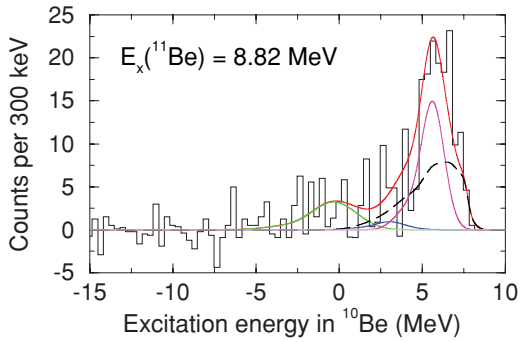

FIG. 3. (Color online) The ^{10}Be excitation energy spectrum produced for the decay of the 8.82-MeV excited state of ^{11}Be. The data is fitted with peak line shapes and a smooth polynomial background. The dashed line represents the events in which the 8.82-MeV state neutron decayed to either the 7.371- or 7.542-MeV ^{10}Be states, which subsequently neutron decayed to the ground state of ^{9}Be.

is shown as a dashed line in Fig. 3. It should be noted that the line shape is not significantly different for the 7.371- and 7.542-MeV decay paths. The state has a substantial width for decay via the sequential emission of two neutrons as well as a strong branch for decay to a ^{10}Be state (or combination of states) at ∼6 MeV. The decay branch to the ground state and the 2^+_1 state are weak and are given as upper limits in Table I.

Table II shows the branching ratios for the neutron decay of various ^{11}Be states taken from the β-delayed neutron decay spectroscopy measurement of ^{11}Li by Hirayama *et al.* [27]. The two sets of measurements are broadly consistent with a few exceptions.

The branching ratios for the 3.96-MeV state do not agree with the current measurement. The present data indicate a stronger decay branch to the ground state of ^{10}Be. Due to the large number of ambiguities in the β-delayed neutron decay spectroscopy method as opposed to the current method, it is suggested that those calculated by Hirayama *et al.* [27] may not be correct for this state. We note that the branching ratios of Hirayama *et al.* [27] cannot be reproduced even if some contribution from the proposed branching ratio of the 3.89-MeV state were to be included in the present data. The neutron decays to the ^{10}Be ground state for the 5.24- and 8.82-MeV states were not observed in Refs. [24,25,27]. The decay of the 8.82-MeV state to the 2^+ state was also not observed in Refs. [24,25,27], consistent with the present observations.

A. Decay widths

An estimate of the theoretical decay widths of the various decay channels were calculated using R-matrix penetrabilities [34]. For neutron decay from an initial ^{11}Be state feeding a ^{10}Be final state, the decay width is given by

$$\Gamma_{^{10}\mathrm{Be}[J_f]} = \sum_{j_n \ell_n} \Gamma^{J_i}_{J_f j_n \ell_n} \tag{4}$$

Here $\Gamma^{J_i}_{J_f j_n \ell_n} = 2\gamma^2 P_\ell$, where P_ℓ is the penetration factor of Ref. [34] (which includes a phase-space factor) and γ^2 is the reduced width. For the purpose of comparison γ^2 has been assumed to be 1 MeV and a radius of 4.4 fm was used in the calculation of the penetrabilities. J_i is the total angular momentum of the parent nucleus and J_f is the angular momentum of the daughter nucleus. The permissible angular momentum combinations $(j_n \ell_n)$ for the outgoing neutron are subject to the condition $\vec{J}_i = \vec{J}_f + \vec{j}_n$ and ℓ_n is either even or odd depending on the transition. The decay branches were calculated for each allowed neutron decay channel of the excited ^{11}Be states of interest. The ratios of the decay branches associated with two different decay channels were then calculated over a range of J^π_i values.

The decay-branch ratio for the neutron decay of ^{11}Be* to the ^{10}Be[0^+] ground state as a fraction of the neutron decay to the 2^+ first excited state is given by

$$R = \frac{\Gamma_{^{10}\mathrm{Be}[0^+]}}{\Gamma_{^{10}\mathrm{Be}[2^+]}}. \tag{5}$$

The ratios were calculated for $J_i = 1/2$ to $9/2$ for both the even- and odd-parity states and are shown in Table III. Also shown are the associated experimental relative branching ratios calculated from the absolute branching ratios of Table I. The theoretical and the experimentally determined ratios were then compared to provide information on the relative reduced widths of the decaying ^{11}Be state.

Table IV shows the ratio of the decay widths for the neutron decay to the 2^+ first excited state as a fraction of the neutron decay to the quartet of state at ∼6 MeV for the 6.72- and 8.82-MeV ^{11}Be states.

TABLE II. The spins, parities, and branching ratios of various ^{11}Be states, taken from the β-delayed neutron decay spectroscopy measurement of ^{11}Li by Hirayama *et al.* [27]. The branching ratios are shown for the neutron decay to the 0^+_1 ground state, the 2^+_1 first excited state, the 6.263-MeV [2^-_1] state, and the 7.371-MeV [3^-_1] state of ^{10}Be.

^{11}Be state (MeV)	J^π	^{10}Be + n			
		0^+_1	2^+_1	2^-_1	3^-_1
3.89	$5/2^-$	0.38 ± 0.01	$0.62^{+0.14}_{-0.21}$		
3.96	$3/2^-$	0.22 ± 0.04	$0.78^{+0.65}_{-0.12}$		
5.24	$5/2^-$		1.00		
7.03	$(5/2^-)$		1.00		
8.82	$3/2^-$			0.25 ± 0.05	0.75 ± 0.02

TABLE III. The theoretical ratios of the neutron decay width of ^{11}Be* to the ^{10}Be[0^+] ground state as a fraction of the neutron decay width to the 2^+_1 first excited state. The ratios are shown for $J_i = 1/2$ to $9/2$ for both even and odd parities. Also shown are the associated experimental relative branching ratios. A comparison between the experimental and theoretical ratios provides information on the relative reduced widths of the decaying ^{11}Be state.

J^π_i	E_x (MeV)			
	3.96	5.24	5.96	6.72
$1/2^-, 3/2^-$	66.21	2.74	2.05	1.67
$5/2^-, 7/2^-$	5.16	0.39	0.37	0.38
$9/2^-$	575.09	0.25	0.14	0.10
$1/2^+$	10096.55	19.08	9.28	5.62
$3/2^+, 5/2^+$	2.03	0.74	0.67	0.62
$7/2^+, 9/2^+$	43.57	0.24	0.18	0.17
Expt.	0.88(0.18)	<0.33	<0.13	<0.20

TABLE IV. The theoretical decay branch ratios for the neutron decay of the 6.72- and 8.82-MeV states of ^{11}Be to the ^{10}Be[2^+] first excited state as a fraction of the neutron decay to the quartet of states at ~6 MeV (2^+_2, 1^-_1, 0^+_2, 2^-_1). The numbers in the brackets represent the strength of the 2^+_2, 1^-_1, 0^+_2, and 2^-_1 decay widths as a percentage of their total width. The ratios are shown for $J_i = 1/2$ to $9/2$ for both the even- and odd-parity states. Also shown are the associated experimental relative branching ratios.

J^π_i	E_x (MeV)	
	6.72	8.82
$1/2^-$	2.12 (15, 85, 01, 00)	0.50 (26, 45, 23, 06)
$3/2^-$	2.12 (15, 85, 01, 00)	0.37 (19, 34, 17, 30)
$5/2^-$	14.05 (97, 03, 00, 00)	0.67 (34, 10, 01, 54)
$7/2^-$	14.05 (97, 03, 00, 00)	1.25 (64, 20, 02, 15)
$9/2^-$	3080.62 (100, 00, 00, 00)	0.96 (12, 01, 00, 87)
$1/2^+$	1.73 (01, 34, 65, 00)	0.27 (09, 27, 39, 25)
$3/2^+$	3.63 (85, 15, 00, 00)	0.79 (45, 26, 07, 23)
$5/2^+$	3.63 (85, 15, 00, 00)	0.79 (45, 26, 07, 23)
$7/2^+$	193.38 (99, 01, 00, 00)	0.80 (25, 03, 00, 72)
$9/2^+$	193.38 (99, 01, 00, 00)	2.68 (84, 09, 00, 06)
Expt.	9.78(4.65)	<0.12

IV. DISCUSSION OF ^{11}Be STATES

In two-neutron transfer reactions four dominant ^{11}Be configurations are expected to be populated. These are the positive-parity states that can be described, in the shell-model limit, as an sd-shell neutron coupled to ^{10}Be(g.s.) or ^{10}Be(2^+), the low-lying negative-parity states that are purely p shell in character and additional negative-parity states based on the $^9\text{Be} \otimes (sd)^2$ configuration. A summary of the ^{11}Be states populated in one- and two-neutron transfer reactions and in the β decay of ^{11}Li is shown in Table V. Also shown are the proposed configurations from Refs. [17,35]. It should be noted that the shell-model orbitals associated with p character form the basis for π-type molecular orbitals and sd-character σ-orbitals.

The 3.96- and 5.24-MeV states are both populated in the β decay of ^{11}Li [21–27] and have been assigned spins of $3/2^-$ and $5/2^-$, respectively [27]. Neither state is populated in one-neutron transfer reactions, whereas they are both populated in two-neutron transfer reactions [17,18]. This confirms their $^9\text{Be(g.s.)} \otimes (sd)^2$ structure. From Table III, for the 3.96-MeV [$3/2^-$] state, the simple barrier penetrability argument indicates that it is 66 times more likely to neutron decay to the ^{10}Be ground state than to the 2^+_1 first excited state, whereas the 5.24-MeV [$5/2^-$] state would neutron decay slightly less to the ground state than to the 2^+_1 state. The

TABLE V. ^{11}Be states populated in $1n$ and $2n$ transfer reactions up to an excitation energy of 11 MeV [15,17,18] and in the β decay of ^{11}Li [27]. Also shown are the proposed configurations from Refs. [17,35].

$2n$ transfer		$1n$ transfer	β decay of ^{11}Li		Configuration
E_x (MeV)	J^π	E_x (MeV)	E_x (MeV)	J^π	
0.00	$1/2^+$	0.00			$^{10}\text{Be(g.s.)} \otimes (s_{1/2})$
0.32	$1/2^-$	0.32	0.32	$1/2^-$	$^{10}\text{Be(g.s.)} \otimes (p_{1/2})$
1.78	$5/2^+$	1.78			$^{10}\text{Be(g.s.)} \otimes (d_{5/2})$
2.69	$3/2^-$	2.69	2.69	$3/2^-$	$^{10}\text{Be}(2^+) \otimes (p_{1/2})$
3.41	$(3/2^-)$		3.41	$(3/2^-)$	$^9\text{Be(g.s.)} \otimes (sd)^2$
3.89	$5/2^-$		3.89	$5/2^-$	$^{10}\text{Be}(2^+) \otimes (p_{1/2})$
3.96	$3/2^-$		3.96	$3/2^-$	$^9\text{Be(g.s.)} \otimes (sd)^2$
5.24	$5/2^-$		5.24	$5/2^-$	$^9\text{Be(g.s.)} \otimes (sd)^2$
5.96	$(5/2^-, 7/2^+)$				
6.72	$(7/2^-)$				$^9\text{Be(g.s.)} \otimes (sd)^2$
7.10			7.03	$(5/2^-)$	
8.04	$(3/2^-, 5/2^-)$		8.02	$3/2^-$	
8.82	$(9/2^-)$		8.82	$3/2^-$	$^9\text{Be(g.s.)} \otimes (sd)^2$
9.23					
10.73	$(11/2^-)$		10.6	$5/2^-$	$^9\text{Be(g.s.)} \otimes (sd)^2$

experimental relative branching ratio is $\Gamma_{0_1^+}/\Gamma_{2_1^+} = 0.88 \pm 0.18$ for the 3.96-MeV state and $\Gamma_{0_1^+}/\Gamma_{2_1^+} < 0.33$ for the 5.24-MeV state. Thus, the 3.96-MeV state has a significantly larger width for decay to the 2_1^+, or a much smaller width for decay to the 0_1^+, than expected from the penetrability calculations. For the 5.24-MeV state the decay to the 2_1^+ is slightly larger, or the decay to the 0_1^+ is slightly smaller, than expected from the penetrability calculations.

The 5.96-MeV state is prominent in two-neutron transfer reactions and is not observed in one-neutron transfer reactions [17,18]. Thus, it does not have a ^{10}Be(g.s.) + n configuration. It is not populated by the β decay of ^{11}Li [21–27] and is therefore either a positive-parity state or a negative-parity state with a spin greater than 5/2. It strongly favors the decay to the 2_1^+ state of ^{10}Be over the decay to the ground state.

The 6.72-MeV state has previously been observed in two-neutron transfer reactions [15,17]. In Ref. [19] it was interpreted as being the $7/2^-$ member of a molecular rotational band built on the 3.96-MeV $[3/2^-]$ state. The spin is unknown, but it is not populated in the β decay of ^{11}Li [21–27] and is therefore either a positive-parity state or a negative-parity state with a spin greater than 5/2. The state is observed to neutron decay to the 2_1^+ first excited state and to a state (or states) of ^{10}Be at ∼6 MeV. The three possible ^{10}Be states, at an excitation energy of ∼6 MeV, are the 2_2^+, 1_1^-, and 0_2^+. However, due to the finite experimental resolution, decays to these individual states were not resolved.

If the spin of the state was firmly assigned and if the branching ratios of the 2_2^+, 1_1^-, and 0_2^+ states at ∼6 MeV were measured individually, barrier penetrability calculations could then be used to provide evidence on the structure of the state. For example, if the state equally decayed to all three of the states at ∼6 MeV, then Table IV could be used to show that for a spin of $7/2^-$ the neutron decay to the ^{10}Be$[2_1^+]$ first excited state is 14.05 times more favorable than to the trio of states at ∼6 MeV. This would suggest that the state decays as one would expect from the barrier penetrabilities. However, if the state decayed only to the 2_1^+ first excited state and the 1_1^- state, then the barrier penetrabilities could be used to show that for a spin of $7/2^-$ the neutron decay to the 2_1^+ state is 468 times more favorable than to the 1_1^- state. In this case the experimental ratio ($\Gamma_{2_1^+}/\Gamma_{1_1^-} = 9.78$) would show that the decay to the 1_1^- is much larger (or the decay to the 2_1^+ much smaller) than expected, indicating that the 6.72-MeV state has a structure similar to that of the 1_1^- state.

The 6.72-MeV state strongly decays to the 2_1^+ state but only weakly decays to the 0_1^+ state. However, the penetrability calculations of Table III show that the state should have a measurable width for decay to the 0_1^+ state. This characteristic is again similar to that of the 3.96- and 5.24-MeV states. This is interesting as the 0_1^+ and 2_1^+ states of ^{10}Be have similar structures [3–5,7,8]. This suggests that all of these three ^{11}Be states may have a similar structure whose wave function has a stronger overlap with the 2_1^+ state than the 0_1^+ state. The commonality of the decay paths would be in general agreement with the interpretation of the three states being members of a molecular rotational band [19] (3.96 MeV $3/2^-$, 5.24 MeV $5/2^-$, and 6.72 MeV $7/2^-$).

The 8.82-MeV state is populated in the β decay of ^{11}Li [21–27] and has been assigned a spin of $3/2^-$ [27]. This is different to Ref. [19], where the state is proposed to be the $9/2^-$ member of a molecular rotational band built on the 3.96-MeV $3/2^-$ state. In the latter instance, the state is proposed to have a ^{9}Be(g.s.) $\otimes (d_{5/2})^2_{4^+}$ configuration that is expected to be strongly populated in two-neutron transfer reactions in accordance with dynamic matching conditions [36], as is experimentally observed. Thus, it is possible that this peak is associated with more than one state and that this region is occupied by both a $3/2^-$ and a $9/2^-$ state.

However, as with the β-decay studies, in the current measurement, the state is observed to have a strong decay branch to a ^{10}Be state (or states) at ∼6 MeV and it is also observed to decay via the sequential emission of two neutrons via either or both of the 7.371- and 7.542-MeV ^{10}Be states. The decay to the four states at ∼6 MeV is unresolved as is the decay to the 7.37- and 7.54-MeV states. However, in the β-delayed neutron decay measurement of ^{11}Li by Hirayama *et al.* [27] the coincident detection of β's, γ's, and neutrons enables the branches to the individual states to be determined. Here, it was found that the state decays to the 6.26-MeV $[2_1^-]$ and 7.37-MeV $[3_1^-]$ states. Hence, the decay branches measured here for the 8.82-MeV state are very similar to those measured in β decay. However, this alone is insufficient to assign the spin and it remains a possibility that the state populated here is a member of the 3.96-MeV band.

By considering only the barrier penetrabilities, Table IV can be used to show that for a spin of $3/2^-$ [27] the ratio for the decay to the 2_1^+ first excited state to the decay to the 2_1^- is 1.23. Experimentally this ratio is less than 0.12. Thus, the decay to the 2_1^- is much larger than expected, or the decay to the 2_1^+ first excited state is much smaller than expected, from the penetrability calculations. In addition, the decay branches to the more compact ^{10}Be ground state is small, if it exists at all. It is also interesting that the state does not decay to the other three states of ^{10}Be at ∼6 MeV. This suggests that the 8.82-MeV state and the 2_1^- and 3_1^- ^{10}Be states may have comparable structures. For example, the 8.82-MeV state has a likely ^{9}Be(g.s.) $\otimes (sd)^2$ configuration and the 2_1^- and 3_1^- states have likely ^{9}Be(g.s.) $\otimes (sd)$ configurations, which are reached by the emission of a neutron from the sd shell. In a description that involves molecular orbitals this would be equivalent to a $(\pi)(\sigma)^2$ configuration in ^{11}Be decaying to $(\pi)(\sigma)$ in ^{10}Be.

This is in agreement with previous theoretical models that have predicted that the 2_1^- and 3_1^- states are members of a molecular rotational band built on the 5.96-MeV 1_1^- state [3–12]. This would suggest that the 8.82-MeV state is also a possible molecular structure. Furthermore, this state lies close to the $2\alpha + 3n$ decay threshold (8.89 MeV). Clearly, a definitive determination of the structure of the negative-parity ^{10}Be states at ∼6 MeV is key to understanding these structures, as is a firm spin assignment of the 8.82-MeV state populated in $2n$ transfer.

Recent calculations performed by Ito *et al.* on the ^{12}Be system indicate that a variety of molecular or cluster structures appear close to the decay threshold [37]. For example, in the $2\alpha + 4n$ system, the ^{4}He + ^{8}He, ^{5}He + ^{7}He, and ^{6}He + ^{6}He

partitions were all found to be important. It is likely that ^{11}Be will have similar features, with the appearance of ^{4}He + ^{7}He and ^{5}He + ^{6}He configurations, which will give rise to cluster bands close to the α-decay threshold. It is possible that the 3.96- and 8.82-MeV $3/2^-$ states are associated with such structures. For example, the covalent exchange of neutrons has been argued to lower the kinetic energy, i.e., increasing the binding energy of the nucleus [3–6]. This may mean that the 3.96-MeV state is associated most strongly with the molecular structure. The appearance of the 8.82-MeV state close to the decay threshold may indicate that the influence of the covalent exchange is diminished, with one or more neutrons located more at one center than the other, and the state has become more a cluster state (as described in Ref. [37]). To summarize, the 3.96-MeV $3/2^-$, 5.24-MeV $5/2^-$, and 6.72-MeV $7/2^-$ states appear to have similar decay properties and thus may form a rotational band.

For the 8.82-MeV state, a $3/2^-$ assignment [27] has been made in the β-decay measurements and it has also been suggested from $2n$ transfer that a state at this energy has spin and parity $9/2^-$ [19] and is a continuation of the 3.96-MeV $3/2^-$ band. Thus, there are two possibilities. First, the states observed in the $2n$ transfer and β decay are different and the similarity of the decay patterns is coincidental. In this case the β decay populates a $(2s_{1/2})^2$ structure ($J^\pi = 3/2^-$) and the $2n$ populates a $(1d_{5/2})^2$ structure ($J^\pi = 9/2^-$). Two-neutron transfer would be better matched to populating d orbitals. The $3/2^-$ state would be a new bandhead and the $9/2^-$ state the continuation of the molecular band. Second, the two states are the same and have $J^\pi = 3/2^-$ as reflected in the decay branches measured here and in Ref. [27]. In either case a state at 8.82 MeV with $J^\pi = 3/2^-$ exists and has most likely a $^{9}\mathrm{Be}_{\mathrm{g.s.}} \otimes (2s_{1/2})^2$ structure.

V. SUMMARY

The two-neutron transfer reaction ^{9}Be(^{16}O, ^{14}O) ^{11}Be[^{10}Be + n] has been used to measure the branching ratios of the excited states of ^{11}Be. The theoretical decay branches of these states have been calculated under the consideration of the R-matrix barrier penetrabilities. Differences between the theoretical and experimental widths have been used to provide information on the relative reduced widths of the states. The decay widths and the structures of the excited states of the ^{10}Be daughter nucleus have been used to predict the structures of the decaying ^{11}Be states.

The 3.96-MeV $3/2^-$, 5.24-MeV $5/2^-$, and 6.72-MeV $7/2^-$ states appear to have similar decay properties and thus may form a rotational band. The 8.82-MeV [$3/2^-$] state has been identified as a likely molecular/cluster bandhead. The 8.82-MeV state has also been identified in β decay of ^{11}Li and has been assigned a halo-type structure. In this instance there appears to be a close connection between molecular/cluster and halo states.

ACKNOWLEDGMENTS

The authors thank the staff members of the Hahn-Meitner-Institut for their assistance in running the experiments. We acknowledge the financial support of the U.K. Engineering and Physical Sciences Research Council (EPSRC). M.F. acknowledges the Alexander von Humboldt foundation for financial support.

[1] B. Buck, H. Friedrich, and C. Wheatley, Nucl. Phys. **A275**, 246 (1977).
[2] J. Hiura and R. Tamagaki, Suppl. Prog. Theor. Phys. **52**, 25 (1972).
[3] W. von Oertzen, Z. Phys. A **354**, 37 (1996).
[4] W. von Oertzen, Z. Phys. A **357**, 355 (1997).
[5] W. von Oertzen, Nuovo Cimento A **110**, 895 (1997).
[6] W. von Oertzen and H. G. Bohlen, C. R. Phys. **4**, 465 (2003).
[7] Y. Kanada-Eńyo, H. Horiuchi, and A. Doté, J. Phys. G **24**, 1499 (1998).
[8] Y. Kanada-Eńyo, H. Horiuchi, and A. Doté, Phys. Rev. C **60**, 064304 (1999).
[9] M. Freer, E. Casarejos, L. Achouri, C. Angulo, N. I. Ashwood, N. Curtis, P. Demaret, C. Harlin, B. Laurent, M. Milin *et al.*, Phys. Rev. Lett. **96**, 042501 (2006).
[10] Y. Ogawa, K. Arai, Y. Suzuki, and K. Varga, Nucl. Phys. **A673**, 122 (2000).
[11] N. Itagaki and S. Okabe, Phys. Rev. C **61**, 044306 (2000).
[12] N. Itagaki, S. Hirose, T. Otsuka, S. Okabe, and K. Ikeda, Phys. Rev. C **65**, 044302 (2002).
[13] H. G. Bohlen, T. Dorsch, T. Kokalova, W. von Oertzen, C. Schulz, and C. Wheldon, Phys. Rev. C **75**, 054604 (2007).
[14] Y. Kanada-Eńyo, H. Horiuchi, and A. Ono, Phys. Rev. C **52**, 628 (1995).
[15] F. Ajzenberg-Selove, R. F. Casten, O. Hansen, and T. J. Mulligan, Phys. Lett. **B40**, 205 (1972).
[16] F. Ajzenberg-Selove, Nucl. Phys. **A506**, 1 (1990).
[17] G.-B. Liu and H. T. Fortune, Phys. Rev. C **42**, 167 (1990).
[18] H. G. Bohlen, A. Blazevic, R. Kalpakchieva, B. Gebauer, S. M. Grimes, T. N. Massey, M. Milin, W. von Oertzen, C. Schulz, T. Kokalova *et al.*, *Proc. Int. Symp. on Exotic Nuclei, Lake Baikal, Russia* (World Scientific, Singapore, 2002), pp. 453–470.
[19] H. G. Bohlen, W. von Oertzen, A. Blazevic, B. Gebauer, S. M. Grimes, R. Kalpakchieva, T. N. Massey, and S. Thummerer, Phys. At. Nucl. **65**, 603 (2002).
[20] N. K. Timofeyuk and P. Descouvemont, J. Phys. G **22**, L99 (1996).
[21] F. Sarazin, J. S. Al-Khalili, G. C. Ball, G. Hackman, P. M. Walker, R. A. E. Austin, B. Eshpeter, P. Finlay, P. E. Garrett, G. F. Grinyer *et al.*, Phys. Rev. C **70**, 031302(R) (2004).
[22] M. J. G. Borge, H. Fynbo, D. Guillemaud-Mueller, P. Hornshøj, F. Humbert, B. Jonson, T. E. Leth, G. Martínez-Pinedo, T. Nilsson, G. Nyman *et al.*, Phys. Rev. C **55**, R8 (1997).
[23] D. J. Morrissey, K. N. McDonald, D. Bazin, B. A. Brown, R. Harkewicz, N. A. Orr, B. M. Sherrill, G. A. Souliotis, M. Steiner, J. A. Winger *et al.*, Nucl. Phys. **A627**, 222 (1997).
[24] N. Aoi, K. Yoneda, H. Miyatake, H. Ogawa, Y. Yamamoto, E. Ideguchi, T. Kishida, T. Nakamura, M. Notani, H. Sakurai *et al.*, Z. Phys. A **358**, 253 (1997).

[25] N. Aoi, K. Yoneda, H. Miyatake, H. Ogawa, Y. Yamamoto, E. Ideguchi, T. Kishida, T. Nakamura, M. Notani, H. Sakurai *et al*., Nucl. Phys. **A616**, 181c (1997).
[26] H. O. U. Fynbo, M. J. G. Borge, J. Cederkall, S. Courtin, P. Dessagne, B. Jonson, G. Le Scornet, T. Nilsson, G. Nyman, E. Poirier *et al*., Nucl. Phys. **A736**, 39 (2004).
[27] Y. Hirayama, T. Shimoda, H. Izumi, A. Hatakeyama, K. P. Jackson, C. D. P. Levy, H. Miyatake, M. Yagi, and H. Yano, Phys. Lett. **B611**, 239 (2005).
[28] A. G. Drentje, H. A. Enge, and S. B. Kowalski, Nucl. Instrum. Methods **122**, 485 (1974).
[29] C. A. Wiedner, M. Goldschmidt, and D. Rieck, Nucl. Instrum. Methods **105**, 205 (1972).
[30] M. Löffler, H. J. Scheerer, and H. Vonach, Nucl. Instrum. Methods **111**, 1 (1973).
[31] H. G. Bohlen, R. Kalpakchieva, A. Blazevic, B. Gebauer, T. N. Massey, W. von Oertzen, and S. Thummerer, Phys. Rev. C **64**, 024312 (2001).
[32] P. J. Haigh, N. Ashwood, T. Bloxham, N. Curtis, M. Freer, P. McEwan, D. Price, V. Ziman, H. Bohlen, T. Kokalova *et al*., Phys. Rev. C **78**, 014319 (2008).
[33] H. G. Bohlen, R. Kalpakchieva, W. von Oertzen, T. N. Massey, B. Gebauer, S. M. Grimes, T. Kokalova, A. Lenz, M. Milin, C. Schulz *et al*., Nucl. Phys. **A734**, 345 (2004).
[34] A. M. Lane and R. G. Thomas, Rev. Mod. Phys. **30**, 257 (1958).
[35] D. J. Millener, Nucl. Phys. **A693**, 394 (2001).
[36] D. M. Brink, Phys. Lett. **B40**, 37 (1972).
[37] M. Ito, N. Itagaki, H. Sakurai, and K. Ikeda, Phys. Rev. Lett. **100**, 182502 (2008).